

SUNON®

MagLev Motor Technology
Win IEEE/IAS & CEFC Recognition

2004 IEEE/IAS & CEFC

MagLev Technical Theory Paper Release



Sunon Fan & Blower

Sunonwealth Electric Machine Industry Co., Ltd.
www.sunon.com

As a global leader of total thermal solution, Sunonwealth Electric Machine Industry Co., Ltd. (Sunon) has long been committed to offering nothing but the best products to the cooling industry. After investing significant funds and manpower, Sunon debut MagLev Motor Fan in the fourth quarter of 1999, the world's first-ever cooling fan are zero friction and no contact between the shaft and the bearing during operation.

Immediately following its launch, Sunon's MagLev Motor Fan became the favorite of large vendors around the world, due to its superior features such as low noise, high temperature endurance and super long life. As a cooling fan, its performance was evident from nearly 100,000,000 units being sold in its limited history, as well as orders from around the world.

In addition to receiving recognition from our customers, Sunon's MagLev Motor has its innovative underlying theory introduced to the academe in 2004, when Dr. Cheng-Tsung Liu and Dr. Tsung-Shiun Chiang – both from National Sun Yat-Sen University in Kaohsiung, Taiwan – and Alex Horng - Sunon's president – conducted a study entitled as “Three-dimensional Force Analyses of an Axial-flow Radial-flux Permanent Magnet Motor with Magnetic Suspension” to reason its superiority and published papers on IEEE (Institute of Electrical and Electronics Engineers) annual meetings.

Two papers were published on two IEEE annual meetings, including CEFC 2004 at Seoul, Korea in June 2004 and IEEE/IAS2004 Annual Meeting at Seattle, USA in October 2004, giving a comprehensive evaluation on the cooling fan in which the MagLev design was introduced. Results from actual examination were included to confirm that a motor fan consolidating Sunon's MagLev design would create a stable guidance force which absorbed the shaft in 360° direction, thereby minimizing the vibration effects that the rotor might introduce at any of its operational positions, and alleviating the radial force applied on the connecting bearing system. An adaptive magnetic equivalent circuit model was used to conduct the three-dimensional static/quasi-dynamic force analysis, deducting the result that Sunon's MagLev Motor Fan could run more stably and reliably than conventional motors did.

Recognized by engineers and scholars on the meetings, both papers ascertained how perfect that Sunon's MagLev design was and how it had contributed to the motor design. Here we recommend you to have an insight look on this innovative invention, which is well recognized by the global industry and academe.

Please see the attached for the full text papers presented by Dr. Cheng-Tsung Liu, Dr. Tsung-Shiun Chiang, and Mr. Alex Horng on CEFC 2004 and IEEE/IAS 2004 Annual Meeting.

- Attachment 1 : CEFC 2004
-- The Eleventh Biennial IEEE Conference on Electromagnetic Field Computation
Date : June 6-9,2004 Place : Sheraton Grande Walkerhill Hotel, Seoul, Korea.
Subject : *Three-dimensional Flux Analysis and Guidance Path Design of an Axial-flow Radial-flux Permanent Magnet Motor*

- Attachment 2 :IEEE/ IAS 39th Annual Meeting
Date : October 3-7,2004 Place :Weatin Hotel, Seattle, Washington, USA
Subject : *Three-dimensional Force Analyses of an Axial-flow Radial-flux Permanent Magnet Motor with Magnetic Suspension*

Note: *CEFC 2004 web site : <http://www.cefc2004.com>
 *IAS 39th web site: <http://ewh.ieee.org/soc/ias/ias2004/index.htm>

Three-dimensional Flux Analysis and Guidance Path Design of an Axial-flow Radial-flux Permanent Magnet Motor

Cheng-Tsung Liu¹, Tsung-Shiun Chiang¹, and Alex Horng²

¹Department of Electrical Engineering, National Sun Yat-Sen University
Kaohsiung, Taiwan 80424, E-mail: liu@mail.ee.nsysu.edu.tw, b8731036@student.nsysu.edu.tw

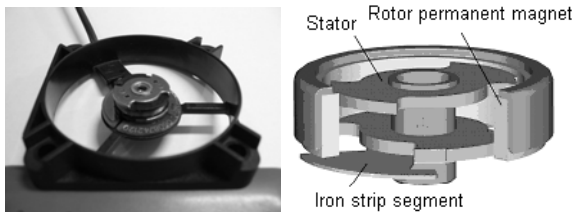
²Sunonwealth Electric Machine Industry Co., Ltd.
Kaohsiung, Taiwan 802, E-mail: alex@email.sunon.com.tw

Abstract - This paper will provide a detailed field analysis of a specially designed axial-flow radial-flux permanent magnet motor for cooling fan applications. By implementing an iron strip segment at the stator base, this motor can provide a stable guidance force in its axial direction, such that the operational vibrations can be minimized and the undesired forces applied onto associated bearing system can be reduced. Supported by dynamic magnetic circuit modeling and three-dimensional finite element analysis, the motor operational fluxes and forces will be analyzed. Results showed that excellent performance and enhanced reliability objectives can all be achieved by this motor.

INTRODUCTION

The axial-flow radial-flux permanent magnet motor along with an iron strip segment, as shown in Fig. 1, has been developed for small-power cooling fan applications [1]. This motor is equipped with only one set of axial stator winding that can supply the desired radial flux through adequate stator pole design, and such structure design is quite promising for applications with limited spaces. With the undesired vibration forces mainly generated in the motor radial direction, the concept is to provide adequate flux path such that a passive magnetic suspension can be established.

An adaptive magnetic equivalent circuit (AMEC), as shown in Fig. 2, has been devised to provide a convenient and



(a) Photograph of the stator base. (b) Conceptual structure of the motor.
Fig. 1. An axial-flow radial-flux permanent magnet motor with a stator iron strip segment.

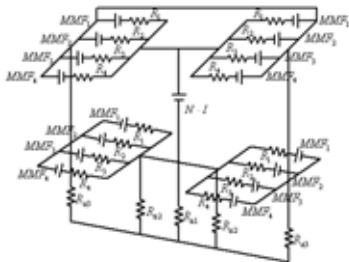


Fig. 2. Magnetic equivalent circuit of the axial-flow radial-flux permanent magnet motor.

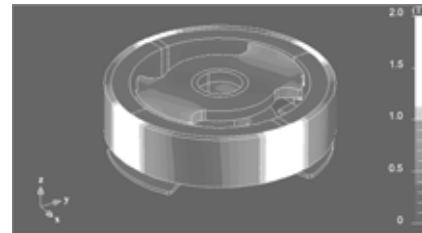


Fig. 3. Operational flux densities at the motor with rated input applied.

accurate mathematical model for the associated performance evaluations at all operational conditions. Supported by 3-D finite element analysis results as shown in Fig. 3, the satisfactory performance and flux guidance effects of the motor can be demonstrated. Results obtained from the AMEC, as shown in Figs. 4 and 5, clearly illustrated that the motor can provide a smoother torques and larger axial forces with same power inputs compared with those without iron strip segment implemented.

REFERENCES

- [1] A. Horng, *Direct current brushless motor of radial air-gap*, US Patent No. 6,538,357, Mar. 2003.
- [2] M. Moallem and G.E. Dawson, "An improved magnetic equivalent circuit method for predicting the characteristics of highly saturated electromagnetic devices," *IEEE Trans. Magn.*, vol. 34, no. 5, Sept. 1998, pp. 3632 – 3635.

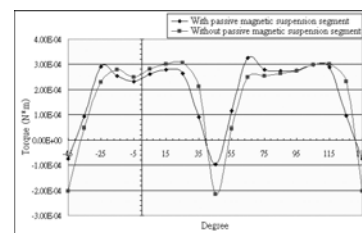


Fig. 4. Operational torques of the motor with rated source inputs.

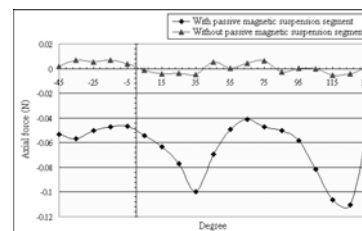


Fig. 5. Axial forces generated onto the rotor permanent magnets.

Three-dimensional Force Analyses of an Axial-flow Radial-flux Permanent Magnet Motor with Magnetic Suspension

Cheng-Tsung Liu, Tsung-Shiun Chiang
 Department of Electrical Engineering
 National Sun Yat-Sen University
 Kaohsiung, Taiwan 80424
 E-mail: ctliu@iee.org

Alex Horng
 Sunonweath Electric Machine Industry Co., Ltd.
 12th Floor, 120, Chung-Cheng 1st Road
 Kaohsiung, Taiwan
 E-mail: alex@email.sunon.com.tw

Abstract This paper will provide a thorough evaluation of a specially designed axial-flow radial-flux permanent magnet motor for cooling fan applications. With a passive magnetic suspension segment implemented, the design objective of this motor is to provide a stable guidance force in its axial direction, such that the vibration effects at the entire rotor operational positions can be minimized and the net radial forces applied onto associated bearing system can be alleviated. Supported by dynamic magnetic circuit modeling and static/quasi-dynamic three-dimensional finite element analyses, the operational forces of such motor, either with or without magnetic suspension, at its respective radial, axial, and tangential directions will all be evaluated. Results show that the motor, which being implemented with a low-cost passive magnetic suspension segment, can supply excellent operational characteristics and thus enhance the operational reliability

Keywords- Adaptive magnetic equivalent circuit; finite element analysis; operational vibration; permanent magnet motor.

I. INTRODUCTION

The axial-flow radial-flux permanent magnet motor along with a passive magnetic suspension segment, as shown in Fig. 1, has been developed for small-power cooling fan applications [1]. This motor is equipped with only one set of axial stator winding that can supply the desired radial flux through adequate stator pole design, and such flat structure is quite promising for applications with limited spaces.

As can be observed from Fig. 1(b), the magnetic fluxes generated from the motor stator winding will first flowing through its stator center shaft, getting out of the stator pole pairs at its top/bottom part, and then coming back to the bottom/top part stator pole pairs after passing through the corresponding rotor magnets. With the pole pairs on the stator top and bottom parts being perpendicular to one another, undesired vibration forces mainly generated in the motor radial direction will be exhibited. The resultant frictions applied onto motor bearing system will certainly generate extra heat and energy losses, and thus reduce the reliability and lifetime of this motor.

The major concerns on cooling fan motor manufactures are low construction/maintenance cost and high operational reliability [2]. In addition to satisfy these construction prerequisites, it is also desired that the overall performance of such motors can preserve their market competitions without implementing complicate sensor and driver control devices. To achieve the aforementioned low cost and simple/reliable structure objectives, as illustrated in Fig. 1(b), the design concept of installing a passive magnetic suspension segment directly on the stator bottom part of the motor has been proposed in one of the commercialized products [1]. This design idea has claimed that a magnetic suspension will be established through the extra flux path being provided. Though it is anticipated that the attraction force between the rotor permanent magnet and the passive magnetic suspension segment will be induced to stabilize the rotor vibrations, intuitively it is also suspected that this segment with high permeability might yield the motor rotational performance.

To evaluate the overall performance of this axial-flow radial-flux permanent magnet motor and investigate the effects contributed from the generated axial force, with and without the passive magnetic suspension segment being implemented, a thorough system electromagnetic field analysis is essential. In addition to the three-dimensional (3-D) finite element analysis (FEA), this paper will present an adaptive magnetic equivalent circuit (AMEC) which can provide a convenient and accurate mathematical model for the related performance evaluations at all of the operational conditions.

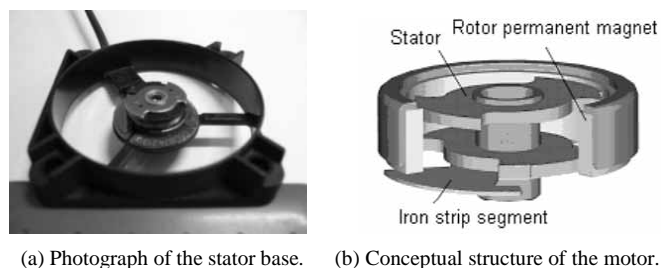


Fig. 1. An axial-flow radial-flux permanent magnet motor with a stator passive magnetic suspension segment.

II. MODELING THE AXIAL-FLOW RADIAL-FLUX PERMANENT MAGNET MOTOR SYSTEM

By referring to the 3-D structure of the motor system as shown in Fig. 1(b), due to the stator pole shape, the cross-sectional view of the motor along with a magnetic equivalent circuit illustrating part of its stator and rotor regions are depicted in Fig. 2. Therefore, based on the physical structure and geometric symmetry of the motor, without the passive magnetic suspension segment, the entire system magnetic equivalent circuit is illustrated in Fig. 3(a). To provide a convenient and accurate mathematical model for the associated performance evaluations at all of the operational conditions, the relative reluctances and magnetomotive forces in the magnetic equivalent circuit must be continuously adjusted according to the rotor positions. Such an adaptive magnetic equivalent circuit (AMEC) can be systematically devised, with the flux flowing through the stator center shaft being expressed as [3]:

$$\phi_c = \phi_{th} + \frac{NI}{R_{th}}, \quad (1)$$

$$\text{with } \phi_{th} = 2 \left(\frac{\text{MMF}_1}{R_{a1}} + \frac{\text{MMF}_2}{R_{a2}} + \frac{\text{MMF}_3}{R_{a3}} + \frac{\text{MMF}_4}{R_{a4}} \right) \text{ and}$$

$$1/R_{th} = 1/R_{a1} + 1/R_{a2} + 1/R_{a3} + 1/R_{a4}.$$

Among which it can be observed that NI is the applied stator winding magnetomotive force, and the branch reluctance R_{ai} , $i=1\sim 4$, is a rotor position dependent function, which can be calculated using the common expression: $R_{ai} = (l_{ai}/\mu_{ai}A_{ai})$.

By referring to Fig. 2 and assuming that the permeability at machine stator and rotor cores are much larger than that at the air gap, it is obvious that the averaged air-gap lengths $l_{a1} = l_{a2}$, $l_{a3} = l_{a4}$, and $l_{a1} > l_{a3}$. While the averaged area of each branch, A_{ai} , $i=1\sim 4$, can be determined by the rotor radius and the corresponding arc spanned at different rotor positions. The equivalent magnetomotive force of permanent magnet at each branch, MMF_i , $i=1\sim 4$, can be determined by the intersection of

material magnetization curve and the operational load line. In here if the thickness of the permanent magnet is l_m , due to structure symmetry, a general assumption that the branch magnetomotive force will be fully applied to its corresponding reluctance can be made, hence the operational load line can be expressed as [4]:

$$\frac{B_m}{H_m} = -\frac{l_m}{A_m R_{ai}}. \quad (2)$$

As for the passive magnetic suspension segment, which being implemented at the bottom part of the stator, it is expected that extra flux paths will be produced. As the air gaps among stator and rotor poles are comparable shorter than the distance between the rotor and the passive magnetic suspension, a reasonable assumption that the major interaction contributed from the rotor permanent magnet will be still taken place among the stator and rotor can be made. The added elements, which can represent the effects of the passive magnetic suspension segment, along with their circuit connections to the original AMEC are thus illustrated in Fig. 3(b).

With all of the magnetic circuit elements and their adaptive scheme being defined, the associated flux and flux density at every branch of the motor system can be derived. Thus, by using virtual works and assuming magnetic linearity, the system coenergy, $W_c(r, \theta, z)$, at different rotor positions and stator magnetomotive forces can be systematically calculated from the AMEC as:

$$W_c(r, \theta, z) \approx 4 \times \sum_{i=1}^4 W_{ci} + W_s, \quad (3)$$

$$\text{with } W_{ci} = \frac{1}{2\mu_0} \int_{r_i}^{r_i+l_{ai}} B_i^2 \cdot A_{ai} dr \approx \frac{1}{2\mu_0} \int_{r_i}^{r_i+l_{ai}} (\phi_i^2 / A_{ai}) dr, \text{ and}$$

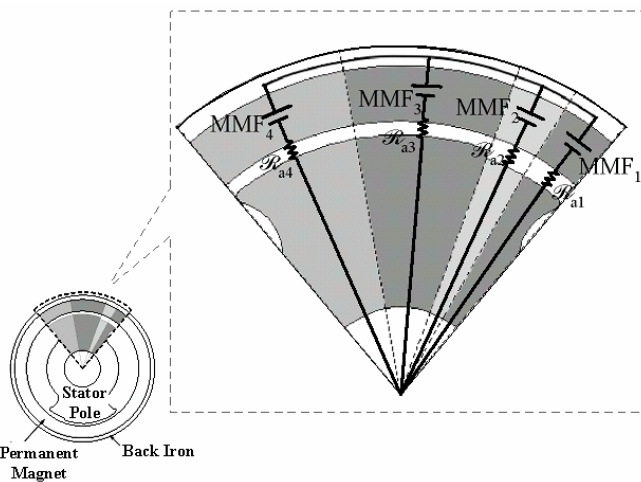
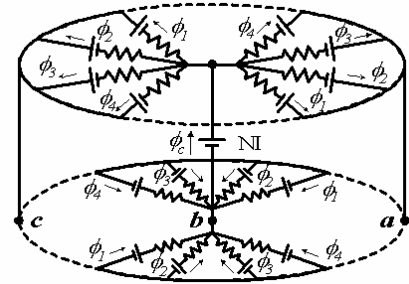


Fig. 2. Cross-sectional view of the motor system and part of the magnetic equivalent circuit representation.



(a) Without the passive magnetic suspension segment implemented.

(b) Extra circuit elements to represent the passive magnetic suspension segment implementation.

Fig. 3. The magnetic equivalent circuit of the axial-flow radial-flux permanent magnet motor system.

$$W_s = \sum_{j=a}^c W_{sj} = \sum_{j=a}^c \frac{1}{2\mu_0} \int_{h_j}^{h_j+z_j} (\phi_{sj}^2 / A_{sj}) dz.$$

Hence the related motor electromagnetic forces and torque can then be expressed as:

$$F_r(r, \theta, z) \approx \lim_{\Delta r \rightarrow 0} [(W_c(r + \Delta r, \theta, z) - W_c(r, \theta, z)) / \Delta r],$$

$$T_e(r, \theta, z) \approx \lim_{\Delta \theta \rightarrow 0} [(W_c(r, \theta + \Delta \theta, z) - W_c(r, \theta, z)) / \Delta \theta], \text{ and}$$

$$F_z(r, \theta, z) \approx \lim_{\Delta z \rightarrow 0} [(W_c(r, \theta, z + \Delta z) - W_c(r, \theta, z)) / \Delta z].$$

In which $F_r(r, \theta, z)$, $T_e(r, \theta, z)$, and $F_z(r, \theta, z)$ are respectively the radial force, the electromagnetic torque, and the axial force of the motor system.

III. 3-D FIELD ANALYSIS AND VERIFICATIONS

To verify the convenience and adequacy of the devised AMEC, a thorough 3-D finite element analysis (FEA) will be performed. By using a commercialized software package [5] and setting appropriate operational conditions, the 3-D finite element meshes of the motor system is depicted in Fig. 4. The physical dimension of the motor is provided in Table I, and the selected mesh sizes of Fig. 4 are illustrated in Table II. The magnetic material used for constructing the stator is H60 with a relative permeability of 6,000, while the material for rotor permanent magnet is bonded ferrite.

By applying a magnetomotive force of 30A·t to the stator winding, without the bottom passive magnetic suspension segment, the flux paths of the motor system are depicted in Fig.

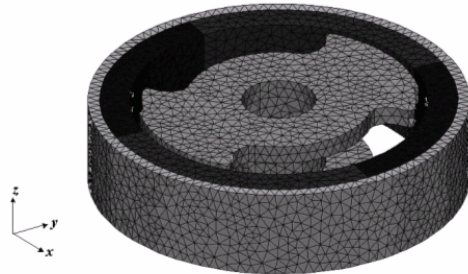


Fig. 4. 3-D finite element meshes of the axial-flow radial-flux permanent magnet motor.

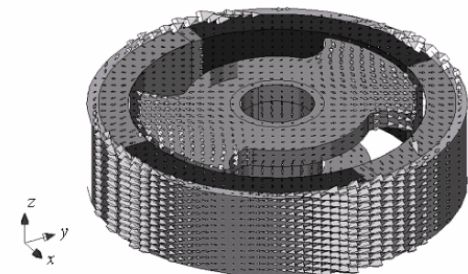


Fig. 5. Magnetic flux paths of the axial-flow radial-flux permanent magnet motor at one rotor position.

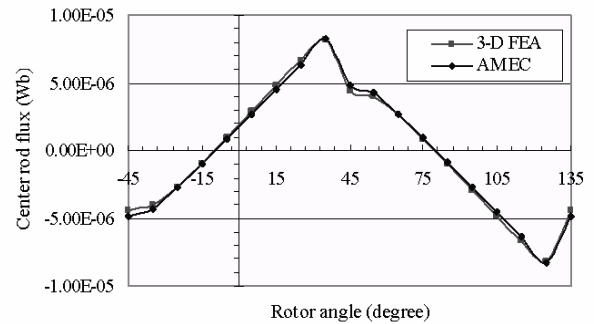
TABLE I
PHYSICAL SIZES OF THE AXIAL-FLOW RADIAL-FLUX PERMANENT MAGNET MOTOR SYSTEM

Symbol	Sizes	Parameter Descriptions
L_s	15.0mm	diameter of stator pole
W_s	10.0mm	diameter of stator axis
H_s	1.0mm	thickness of stator pole
P_s	80°	stator pole arc
P_s'	20°	arc of the stator truncated pole
L_s'	14.5mm	diameter of the stator truncated pole
D_c	4.0mm	inner diameter of stator center rod
L_c	0.5mm	thickness of stator center rod
H_c	4.8mm	height of stator center rod
D_r	15.8mm	inner diameter of rotor
H_r	4.8mm	height of rotor
L_m	1.6mm	thickness of rotor permanent magnet
L_b	0.6mm	thickness of rotor back iron

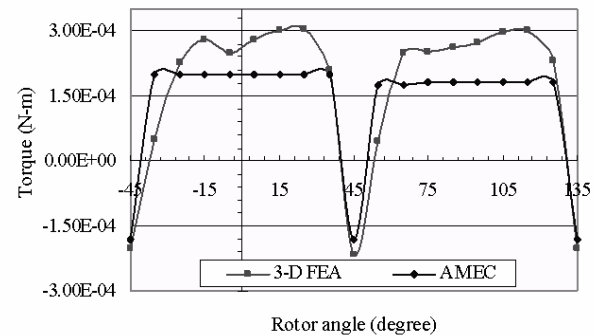
TABLE II
SELECTED MESH SIZES FOR 3-D FEA OF THE MOTOR SYSTEM

Subdomain	Mesh Sizes
outer boundary	5.0mm
outer air	4.0mm
interior air gap	0.2mm
stator pole	0.5mm
rotor permanent magnet	0.5mm
rotor back iron	0.5mm

5. A thorough study has been performed based on both the 3-D FEA and the AMEC schemes, and the flux flowing through the motor center shaft with different rotor positions, as well as the total generated electromagnetic torque of the motor system is depicted in Fig. 6 for comparison. Obviously, from these



(a) Flux ϕ_c at the stator center rod.



(b) Electromagnetic torque T_e .

Fig. 6. Calculated center shaft fluxes and total electromagnetic torques of the motor system with different rotor positions.

investigation results, a reasonable assumption can be made that the AMEC scheme will provide an accurate enough analyzing results in the averaged basis with small enough rotor increment angle. Therefore, it is confident that the predicted operational performance as derived from the AMEC scheme will supply a convenient and satisfactory index for evaluating the overall steady-state characteristics of the motor.

Since the major factor for motor operational vibration is contributed from the unbalanced radial forces applied to the rotor bearing, by using the AMEC and 3-D FEA schemes, the net radial forces of the motor system when the rotor rotates to different positions have been systematically analyzed. These net forces are calculated by subtracting the generated rotor radial forces at certain angles with the ones being 180° mechanically apart. Fig. 7 depicts the schematic diagram that has been used to calculate the net radial forces of the motor system with the rotor rotates to a reference angle of 0°, and the resultant net forces are illustrated in Fig. 8. Theoretically, if there is no vibration effect, the net radial force of the motor at every rotor position must all be zero.

IV. EFFECTS OF THE PASSIVE MAGNETIC SUSPENSION SEGMENT

To alleviate the vibration effects at operations, such that the motor overall reliability can be enhanced and the lifetime can

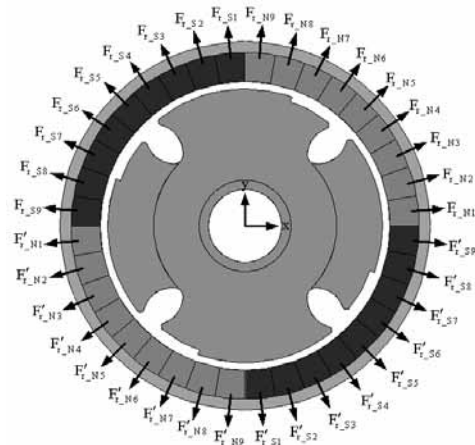


Fig. 7. Schematic diagram for calculating the net radial forces of the motor system with the rotor located at a reference angle of 0°

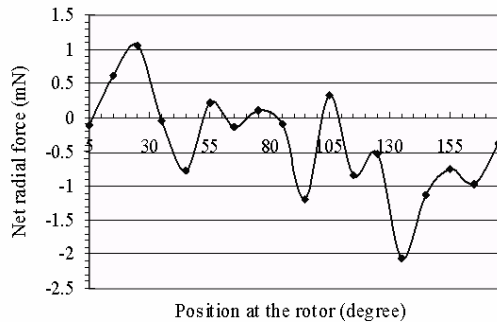


Fig. 8. Calculated net radial forces applied onto the rotor at a reference rotor angle of 0°.

be extended. By implementing a passive magnetic suspension segment at the stator base of the motor, the extra cost compared to the total construction expense of the motor is negligible. While for the motor operational performance, with and without the passive magnetic suspension implemented, the generated electromagnetic torques of the motor are first provided in Fig. 9 for comparison. It can be observed that though slightly more severe notches will be occurred when the rotor being rotated to the positions with negative torque generations, the two torque patterns are closed enough in the overall averaged point of view.

As for the net radial forces of the motor system, with the same operational conditions as that shown in Fig. 8, the generated electromagnetic forces are illustrated in Fig. 10 for comparisons. At first glance, it is obvious the passive magnetic suspension segment will not behaved as the design objective, but will even deteriorate the already exhibited net radial forces. As for ideal case, the net radial forces applied to all the rotor positions must be all zeros. By taking the standard deviations as the statistical indices, the summarized results of the net radial forces at different rotor angles are provided in Table III. The results still showed that a passive suspension segment will provide an up to about 30% larger net radial force to the motor system.

However, for the generated axial forces of the motor system,

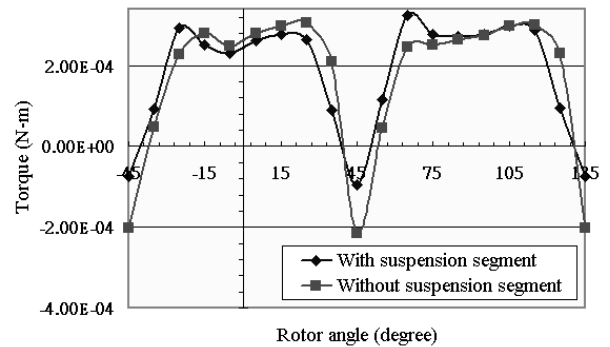


Fig. 9. Calculated total electromagnetic torques of the motor system with different rotor positions.

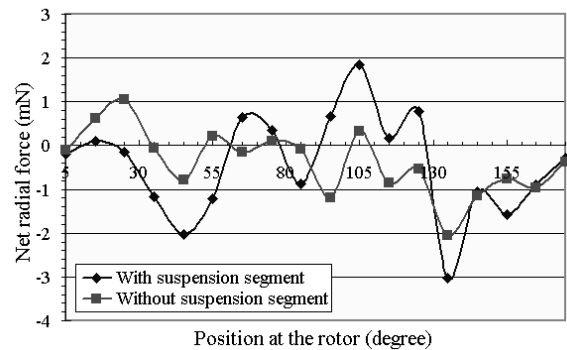


Fig. 10. Calculated net radial forces applied onto the rotor with/without the suspension segment implemented at a reference rotor angle of 0°.

as can be clearly observed from Fig. 11, the additional attracted forces contributed from the passive magnetic suspension segment are clearly illustrated. Since these induced axial forces are in the negative z direction, and they are in the orders of about 50 times of the motor radial forces, the combined force vectors in the motor radial directions will be insignificant. From such observations, the effects of those extra flux paths among the rotor and the passive magnetic suspension segment will supply adequate guidance forces to stabilize the motor operations are evident.

V. CONCLUSION

The operational characteristics of an axial-flow radial-flux permanent magnet motor, with an extra passive magnetic suspension segment implemented on its stator base, for cooling fan applications have been thoroughly investigated. The adequacy and convenience of using the proposed AMEC scheme for continuous/dynamic motor system performance analysis have been verified by 3-D FEA. By introducing extra axial forces to guide the motor rotation with alleviated radial force, the analyzing results clearly illustrated the effects of motor operational stability enhancement through the implementation of passive magnetic suspension segment.

ACKNOWLEDGMENT

The authors wish to express their gratitude to the valuable technical suggestions from Mr. W. Wu and W. Chen of the Sunonwealth Electric Machine Industry Co., Ltd.

REFERENCES

- [1] A. Horng, *Direct current brushless motor of radial air-gap*, US Patent No. 6,538,357, Mar. 2003.
- [2] J.F. Gieras and M. Wing, *Permanent Magnet Motor Technology*, New York, Marcel Dekker, 2002.
- [3] M. Moallem and G.E. Dawson, "An improved magnetic equivalent circuit method for predicting the characteristics of highly saturated electromagnetic devices," *IEEE Trans. Magn.*, vol. 34, no. 5, Sept. 1998, pp. 3632 – 3635.
- [4] C.-T. Liu and K.C. Chuang, "On the design of a disc-type surface-mounted permanent magnet motor for electric scooter application," in *Proc. IEEE IAS 37th Annual Meeting*, vol. 1, Pittsburgh, PA, U.S.A., 2002, pp.377-383.
- [5] Magsoft, *FLUX 3D User's Guide, Version 3.20*, Troy, NY, U.S.A.: Magsoft Corp., Dec. 2000.

TABLE III
STANDARD DEVIATIONS OF THE NET RADIAL FORCES AT DIFFERENT ROTOR REFERENCE ANGLES

Degree	Without Iron Strip Segment	With Iron Strip Segment
0	0.8157	1.1238
30	0.6785	0.8353
60	0.4253	0.4533

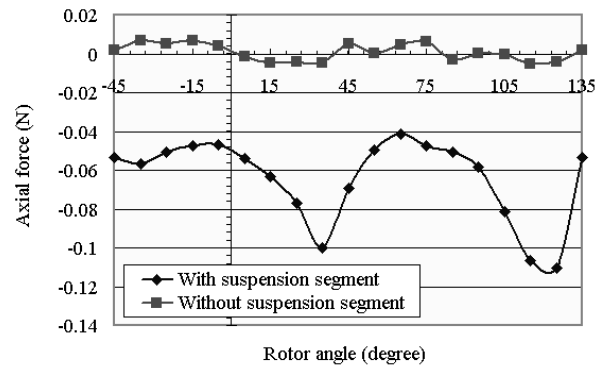


Fig. 11. Calculated total axial forces of the motor system with different rotor positions.